NASA TECHNICAL NOTE

NASA TN D-2804

NASA TN D-2804

A TECHNIQUE FOR OBTAINING PLASMA-SHEATH CONFIGURATIONS AND ION OPTICS FOR AN ELECTRON-BOMBARDMENT ION THRUSTOR

by Eugene V. Pawlik, Paul M. Margosian, and John F. Staggs

Lewis Research Center

Cleveland, Ohio

NATIONAL AERONAUTICS AND SPACE ADMINISTRATION • WASHINGTON, D. C. • MAY 1965

NASA TN D-2804

A TECHNIQUE FOR OBTAINING PLASMA-SHEATH CONFIGURATIONS AND ION OPTICS FOR AN ELECTRON-BOMBARDMENT ION THRUSTOR

By Eugene V. Pawlik, Paul M. Margosian, and John F. Staggs

Lewis Research Center
Cleveland, Ohio

NATIONAL AERONAUTICS AND SPACE ADMINISTRATION

For sale by the Clearinghouse for Federal Scientific and Technical Information
Springfield, Virginia 22151 – Price $2.00

A TECHNIQUE FOR OBTAINING PLASMA-SHEATH CONFIGURATIONS AND ION OPTICS FOR AN ELECTRON-BOMBARDMENT ION THRUSTOR

by Eugene V. Pawlik, Paul M. Margosian, and John F. Staggs

Lewis Research Center

SUMMARY

24376

A technique has been developed for determining the location of the plasma boundaries and the ion trajectories for the accelerator system of an electron-bombardment ion thrustor. The technique consists of using an electrolytic tank and an analog computer to solve Poisson's equation within the region between the ion-chamber and exhaust-beam plasmas with known initial and final plasma potentials. The boundary of the ion-chamber plasma serves as a virtual emitter from which a specified ion current is extracted. The process of matching the boundary conditions, solving Poisson's equation, and finding the ion trajectories is a convergent iterative procedure.

Four two-dimensional cases, representing a range of electrical parameters and ion flows for a fixed accelerator grid geometry, have been solved. From these solutions it is possible to predict experimentally observed trends such as the ion current extraction capabilities of the grid system and the impingement current conditions. High direct impingement was found at high ion flow conditions. Charge-exchange ion focusing toward the region between the holes or the downstream accelerator surface is evident in the solutions.

In addition to comparing predicted trends with experimental data, the accuracy of the solutions was checked with a digital computer program, where the plasma boundary determined by the analog technique was used as a fixed emitter. A comparison between the two-dimensional solutions obtained herein and the axisymmetric situation encountered in actual thrustors was obtained through the use of a digital program.

Author

INTRODUCTION

During the past several years, the electron-bombardment ion thrustor (refs. 1 and 2) has been tested over a wide range of operating conditions. Thus far, electrode design for this device has been primarily empirical (refs. 3 and 4). The ion-optics problem has not been considered readily solvable by rigorous analytical methods (ref. 5) because of the necessity of finding the plasma-sheath configuration as a function of accelerating voltages, electrode geometry, and ion-chamber parameters. Such a calculation would in-

volve the solution of plasma equations for the ion chamber as well as an analytical treatment of the collision processes involved. While such a calculation is (at least in principle) possible, the large number of complex phenomena occurring simultaneously in the chamber make it impractical at present.

An electrolytic tank analog, described in reference 6, has been used to determine ion optics for the case of a well-defined ion emitter surface such as those employed in the contact-ionization thrustor (refs. 7 and 8). One method of using the electrolytic tank for the case of an unknown emitter surface (e.g., a plasma boundary) based on a simplified description of the plasma is presented in reference 9. A more general method based on similar assumptions is presented in this report. This method requires no prior knowledge of the plasma-sheath configuration and differs from previous methods in that variations in space-charge distribution due to changes in the plasma boundary are taken into consideration. The electron and ion temperatures within the plasma of the thrustor are assumed to be small when compared with the accelerating voltages. The conditions that need to be specified are the geometry of the accelerator grid system, the potentials applied to the grids, the plasma potentials, and a current density (i.e., the ion current passing through a single grid hole). With these data, the method yields a solution that gives both the ion optics of the grid system and the shape of the ion-chamber-plasma boundary. In addition, the solution yields the approximate location of the exhaust-plasma boundary or virtual ground, that is, the boundary of the region downstream in which beam neutralization has occurred (ref. 10).

The scale model used with the electrolytic tank in the present investigation consisted of a two-dimensional section of a single hole from a typical accelerator grid system. This model is used to analyze four cases representing a wide range of current densities with constant voltage between the grids.

The accuracy of the solutions was checked by use of a digital computer program, which was capable of obtaining the space-charge-limited ion current from a fixed emitting surface at a specified potential. The checking consisted of using the plasma boundaries obtained by the electrolytic-tank solution as fixed electrode surfaces in the digital program. Another digital computer program was used to compare these two-dimensional results with an axisymmetric solution for the same emitter shape.

THRUSTOR DESCRIPTION

A cutaway view of a typical electron-bombardment ion thrustor is shown in figure 1. The propellant flows through a calibrated restriction between the vaporizer and the flow distributor. After leaving the distributor, the propellant enters the ion chamber. A field winding surrounding the thrustor provides a magnetic field roughly parallel to the axis of the ion chamber. Electrons from a hot cathode bombard the neutral atoms in the chamber, ionizing some of them and thus filling the chamber with a plasma. Ions that diffuse to the screen grid are electrostatically accelerated toward the accelerator grid and ejected from the thrustor. Electrons are added at a downstream location to neutralize the ion beam and form an exhaust plasma. The portion of the thrustor simulated by the analog model is also shown in the figure.

THEORY

The solution to the problem of determining the ion optics for the electron-bombardment ion thrustor consists of finding the ion trajectories as a function of grid geometry, applied voltages, and ion current. In order to determine the ion trajectories, it is necessary to find the plasma sheath or boundary formed behind the screen grid (fig. 1) from which the ions are extracted. An exact solution to this problem would require a detailed analysis of ion-chamber phenomena, a problem of formidable complexity. With the help of suitable assumptions, it is possible to simplify the problem greatly. Agreement of the final results with experimental data obtained by other methods can be used to verify the validity of these assumptions.

The technique presented herein involves solving Poisson's equation ($\nabla^2 V = -\rho/\epsilon_o$) for the potential distribution in the space-charge region between the ionization chamber plasma and the exhaust plasma and fitting this solution to the boundary conditions. (All symbols are defined in the appendix.) The boundary conditions are prescribed by the physical shape, the location, and the potential of the electrodes. For the special case in which a plasma forms one of the boundaries, the condition needed at the plasma-sheath surface is $\nabla V = 0$. This is also the condition at any space-charge limited ion emitting surface. If the plasma potential in both the ion chamber and the exhaust are assumed to be known, the condition $\nabla V = 0$ at these plasma boundaries is sufficient to solve Poisson's equation for any specified ion current by an iterative procedure.

A sketch of the system potentials as a function of distance is shown in sketch (a). The plasma boundary or sheath is assumed to be located at the point where the potential gradient approaches zero. The boundary for the chamber plasma serves as an emitter from which a specified ion current is extracted. The simplified model in sketch (a) is justified if (as is usual for an ion thrustor) the random electron and ion energies are negligible compared with the accelerator potential difference.

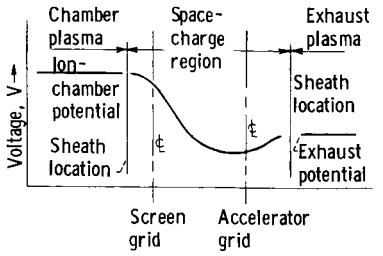

(a)

The potential of the ion-chamber plasma is assumed to be constant at a value very close to that of the screen grid. In reality, the plasma potential may be close to the anode potential (25 to 50 V above that of the screen), and the potential within the plasma may vary by several volts across the ion chamber (ref. 11); however, these uncertainties in the plasma potential, a maximum of about 50 volts, are small compared with the voltage between grids (normally above 3000 V). The exhaust plasma is assumed to be at ground potential.

In the present study, the system was further simplified by considering only a two-dimensional model of a single hole in the accelerator grids. Quantitative differences between calculated and experimental results would therefore be expected.

ELECTROLYTIC TANK ANALOG

The electrolytic tank, complete with space-charge-simulation pins and the model used for the cases presented in this report, is shown in figure 2. It consists of an accurately leveled plastic tray 16 inches wide, 30 inches long, and 2 inches deep. Current-injection pins, which provide space-charge simulation (refs. 12 and 13), project from the floor of the tray. Stainless-steel electrodes, scaled in size from actual grids in an ion thrustor, are maintained at potentials that are also scaled from typical thrustor potentials. When the tray is filled to the proper level with electrolyte, electric fields are set up by the electrodes and space-charge-simulation pins. These fields are scaled replicas of those in the accelerator system of the actual thrustor. The x and y components of these fields are measured by the field-sampling probe (fig. 2), and the resulting signals are fed to an analog computer. The analog computer solves the equations of motion for the ion being considered (mercury in this case) generating a signal to the servomotors that drive the field-sampling probe along the path an ion would take within the electric field. An X-Y plotter follows the motion of the field-sampling probe, recording the determined trajectories. Timing signals are introduced at the plotter. The spacing between the resulting timing marks is a measure of the velocity of the ion. By reprograming the analog computer, it is also possible to plot equipotentials and field lines. A more detailed description of the electrolytic tank is given in reference 6.

The electrode model used for this study is shown mounted in the electrolytic tank in figure 2. The stainless-steel electrodes labeled screen and accelerator grids are scaled to 32 times the actual size from a set of grids used in a typical thrustor. The dimensions of the grid system simulated are: hole diameter, 0.476 centimeter; plate separation, 0.153 centimeter; grid thickness, 0.085 centimeter; and web thickness (edge to edge distance between adjacent holes), 0.269 centimeter. The space-charge pins were located 2 centimeters apart, which represents 0.063 centimeter in the thrustor. The model used represents a two-dimensional section from the grid system as shown in figure 1. The plastic strips labeled midhole boundary (fig. 2) simulate the field conditions of an array of holes (i.e., the strips are placed on the axis of symmetry of the grids, fig. 1).

The electrode to the left of the screen grid in figure 2, labeled ion-chamber plasma represents a region of constant potential within the plasma of the ion chamber and is held at the same potential as the screen grid. This electrode is arbitrarily located about 3 hole diameters from the grid system in order to guarantee that its shape and location will have a negligible effect on the final solution. In all cases the actual sheath boundary is located much closer to the screen grids than this ion-chamber-plasma electrode.

The electrode to the right of the accelerator grid in figure 2 labeled beam plasma represents a region of constant potential within the exhaust plasma downstream of the thrustor in which beam neutralization has taken place. It is maintained at or near ground potential. As in the case of the upstream plasma electrode, this electrode is located about 3 hole diameters from the grid system.

PROCEDURE

In order to provide a measure of the flexibility of the technique used in the solution of the optics problem, four cases, representing a wide range of electrical parameters, were studied. In all cases the grid geometry was the same. The electrical parameters used for the four cases are given in table I. The primary emphasis was in determination of the location of upstream or ion-chamber plasma boundary. The downstream plasma boundary or virtual ground can be located only approximately in the final solution due to the limitations of the equipment used.

The iterative technique used in locating the plasma boundary can be demonstrated by following a specific case, step by step, to a converged solution. Case 1 of table I has been selected for illustrative purposes. This case corresponds to an ion-beam current of about 50 milliamperes from a 10-centimeter-diameter thrustor. It is known from experimental data that 50 milliamperes is roughly one-fourth of the maximum current attainable with the specified grid geometry and applied voltages (ref. 3).

Laplace Solution

To begin the procedure, it is necessary to obtain the Laplace (space-charge-free) solution. This was done by starting trajectories from the electrode representing the ion-chamber plasma within the ion chamber and allowing them to fall through the fields set up by the electrodes alone. The results of this process are shown in figure 3. The Laplace solution is used as the initial approximation to calculate space charge, as described in the following section.

Calculation of Space Charge

For the first step of the calculation (and only the first), the current is assumed to be uniformly distributed over the ion-chamber-plasma electrode. For this initial estimate of the plasma boundary, each trajectory represents the same fraction of the total current passing through the hole, because the starting points are equally spaced. If the current represented by each trajectory and the ion velocity are known, it is possible to calculate a space-charge distribution by the technique discussed in reference 6. Briefly, this technique is as follows.

A transparent grid overlay is superimposed over the trajectories obtained for the Laplace solution. This grid is laid out with a space-charge-simulation pin in the center of each square. Stream-tube boundaries are then sketched midway between adjacent trajectories. The current represented by a given trajectory is considered to be uniformly distributed across the width of this stream tube. The space charge to be simulated in each square of the grid is determined by current in each stream tube, the time that the ions spend in the square, and the number of stream tubes intercepting the square.

Once the space charge to be simulated in a given square has been deter-

mined, the current to be injected by the appropriate space-charge-simulation pin can be obtained from a calculation involving the geometric scale factor, the voltage scale factor, and the conductivity of the electrolyte, as discussed in detail in references 6, 12, and 13.

First Iteration

The space-charge distribution determined from the Laplace solution is added by the space-charge-simulation pins. The pin currents are set at the downstream end (right end of the model in fig. 2) first. The remaining pin currents are then set, advancing row by row toward the grid system. As the grids are approached, the potential at the surface of the electrolyte is monitored continuously by the potential probe. This process is continued until a reasonably regular equipotential line with a voltage near that of the screen grid appears. When this occurs, no more pins are set. The resulting potential distribution along the centerline of the model is shown in figure 4, as the curve labeled iteration 1. The equipotential line, which represents the first approximation to the plasma sheath, is shown as iteration 1 in figure 5. (Subsequent iterations are also included in these figures.)

Ideally, the entire region behind the equipotential line (fig. 5) would be at the same potential, simulating a plasma region. The potential gradient at this line would be zero, and there would be no space-charge-simulation pins set upstream of this line. In practice, this situation is not approached for several iterations. In addition, it is necessary for the investigator to exercise some judgment in deciding when to stop setting pin currents. It must be kept in mind that the plasma-sheath boundary should be located relatively near the screen grid and should be symmetric about the centerline of the hole. A certain amount of adjustment proves necessary.

The first approximation to the plasma-sheath boundary is used as a source line, and trajectories are again plotted using the electrolytic tank analog. This approximation to the plasma boundary and the trajectories resulting from it (shown in fig. 6) provide a first approximation to the solution of the ion-optics problem.

Second Iteration

The next step is to determine a new space-charge distribution based on the trajectories found in the first iteration (fig. 6). It is necessary to determine the current represented by each trajectory before proceeding. Because it is known that the total current passing through the hole is the space-charge-limited current from the plasma sheath, the current represented by each trajectory is calculated on the basis of Child's law. This is done as described in references 6 and 14. Outlined briefly, the procedure is as follows: An equipotential line lying very close to the previous approximation to the plasma boundary is plotted. These two adjacent equipotentials are then regarded as a series of plane diodes, divided as shown in sketch (b).

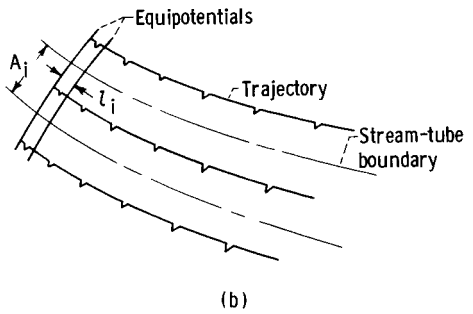

(b)

The typical elementary stream tube has a distance l_i between the adjacent equipotentials measured along the stream tube and an area proportional to A_i, the curvilinear distance between the stream-tube boundaries measured along the upstream equipotential. From Child's law the current represented by a given stream tube must be proportional to $A\,\Delta V^{3/2}/l^2$. Since the total current J_B leaving the plasma boundary is specified, the current represented by a given trajectory is

$$J_i = \frac{A_i/l_i^2}{\sum_1^N A_i/l_i^2} J_B$$

where N is the total number of stream tubes. If the currents in the stream tubes are known, the space-charge distribution and the resulting pin currents can be obtained by the same calculation used previously.

The calculated pin currents are set in the same fashion as the first iteration, and the potential on the surface of the electrolyte is monitored as before. In all four cases studied in this investigation, it was found that, after all the calculated pin currents had been set, an equipotential line with the assumed plasma potential did not appear. This situation indicates that there is insufficient space charge in the vicinity of the grid system and that the actual plasma boundary must therefore be located farther upstream than the approximation obtained in the first iteration, but its exact location becomes arbitrary. The method used to locate the boundary in this study was to set additional space-charge-simulation pins upstream of those for which calculated values were available until the desired equipotential appeared. The magnitudes of the currents injected by these pins were generally taken to be the same as those for the last two or three rows of pins having calculated settings. Some additional adjustment of pin currents was necessary in order to assure symmetry of the plasma boundary about the centerline of the grid hole and approach the condition $\nabla V = 0$ at the boundary. The approximation obtained in this fashion is shown in figure 5 (curve 2).

Third and Subsequent Iterations

Once a new approximation to the plasma boundary has been located, the procedure is continued as before. An equipotential near the sheath voltage is located, trajectories are determined, the current represented by each stream tube is found from Child's law, and a new space-charge distribution is calculated. Pin currents are set using the procedure outlined for the first iteration or for the second iteration, whichever proves appropriate. The centerline potential distributions for the first four iterations are shown in figure 4. Iteration 4 required adjustment because the centerline potential distribution did not meet the upstream boundary condition (a situation similar to that described for iteration 2). The distribution before adjustment is labeled 4a,

while that after the adjustment is labeled 4. All the approximations to the plasma-sheath boundary from the first iteration to solution are shown in figure 5 for the sample case. After several iterations, it is no longer necessary to make any sort of arbitrary adjustment. This is one indication that a solution is being approached.

Convergence Criteria

The conditions demanded of a solution were as follows:

(1) The final approximation to the plasma boundary should be located very nearly in the same position as the previous approximation. The separation between the two approximations should be less than half the spacing between space-charge-simulation pins (2 cm).

(2) The condition $\nabla V = 0$ must be very nearly satisfied in the vicinity of the final approximation to the boundary.

(3) The trajectories in the final approximation should be very nearly the same as those in the previous approximation.

(4) No arbitrary adjustment of pin current settings should be necessary for the final solution, and a minimum of such adjustment should have been needed in the previous approximation.

(5) There should be a minimum of pins set upstream of the plasma-sheath boundary. (Ideally there should be none because a plasma is electrically neutral. In practice, there will usually be a small number of pins set behind the boundary because of the finite spacing between the pins.)

(6) The sheath boundary should be nearly symmetric about the centerline of the model.

Limitations of Solution

The solution obtained by the process just outlined is a fairly accurate one (see RESULTS AND DISCUSSION) in all regions except near the screen grid, because an equilibrium sheath representing a voltage drop of up to 50 volts exists between the screen grid and the plasma in an actual thrustor. One of the assumptions in establishing the model of the system was that the plasma and the screen grid were at the same potential; however, the existence of this sheath must be recognized, and this portion of the plasma boundary is shown as a dashed line in the final solutions. This region of uncertainty is a sufficiently small portion of the plasma boundary that it does not introduce significant errors.

Possible Variations in Procedure

Because of the arbitrary nature of portions of the procedure, some vari-

ation is possible. An area with considerable lattitude is the method of starting the problem. The initial set of trajectories need not be started from a flat surface far from the accelerator grids as was done in this study. Other starting points may be used, for example, a curved surface near the screen grid. In addition, it is not necessary to start with a Laplace solution. Any desired initial space charge may be simulated. A judicious choice of conditions for the initial run could substantially decrease the number of iterations required to arrive at the converged solution.

The velocity of the ions arriving at the ion-chamber-plasma boundary were assumed to be negligible for the results presented. The effects of both the drift velocity and the direction of the ions within the plasma could be evaluated by adding an initial velocity and direction to the potential probe by means of the analog computer program.

Determining Downstream Boundary

Ideally, the boundary of the downstream plasma region (at ground potential) could be obtained by the same procedure as was used to locate the upstream boundary. Space-charge-simulation pins would be set starting somewhere near the accelerator grid and working in both directions, while continuously monitoring the potential at the surface of the electrolyte, searching for approximations to both boundaries.

In practice it was not feasible to locate the downstream plasma boundary accurately in this manner because of the extremely low potential gradients in this region. These low gradients made accurate measurements impossible with the present equipment. The best that could be done was to set the pin currents in the fashion previously described, find a converged solution for the upstream sheath, and locate an equipotential line corresponding to ground potential. The centerline potential distribution exhibits a slight hump downstream of this line (fig. 4). This hump is due to a space charge that would be neutralized by electron backflow in a real thrustor. An estimate of the accuracy of the boundary thus located was obtained for the sample case by turning off the space-charge-simulation pins located farther downstream, thus making this an approximately equipotential region. As a result, the equipotential corresponding to the boundary of the virtual ground shifted position by a distance comparable to the spacing between space-charge-simulation pins. Hence, the location of this downstream boundary must be considered no more accurate than this shift distance.

RESULTS AND DISCUSSION

The technique described was used to carry through a total of four cases to converged solutions. The electrical parameters for these cases are presented in table I. The total accelerating voltage was kept constant at 3333 volts for all cases. The ratio of net to total accelerating voltage was 0.8 for cases 1 and 2 and 0.5 for cases 3 and 4. The current J_B listed within the table corresponds to the total ion beam current that would normally be

expected from a 10-centimeter-diameter thrustor with a 50-percent open-area electrode system, if each hole delivers an equal contribution to the beam and no direct impingement exists. A uniform ion density is seldom achieved, however, and the values of beam current are included only as relative figures of merit. A beam current of about 0.128 ampere represents an optimum operating condition for this size thrustor from the standpoint of efficient source operation (ref. 15) and reasonable accelerator lifetimes (ref. 16). The first case (fig. 7) presents the accelerator optics at a beam current less than half the preceding conditions: two cases (figs. 8 and 9) are considered near these conditions. The last case (fig. 10) presents the accelerator optics at a beam current considerably above this level. The trends predicted by these solutions and a comparison with previously reported experiments are discussed in the following section.

Predicted Ion Optics

The effect of various electrical parameters on the locations of the plasma boundaries and the resulting ion optics can be seen by comparing the four solutions. Many of the results obtained in these solutions can be compared with experimental data.

Effects of ion current. - A comparison of cases 1 and 2 (figs. 7 and 8) shows that, for constant accelerating voltages, the ion-chamber-plasma boundary becomes flatter as the current is increased. The ion paths are focused through a small portion of the downstream grid hole in the low current solution (case 1), and through a much larger portion of this area in the higher current solution (case 2). Cases 3 and 4 (figs. 9 and 10) show a continuation of this trend for a lower ratio of net to total accelerating voltages. The highest current (case 4) results in a convex plasma boundary, severe beam defocusing, and a very high direct impingement.

The current that actually passes through the accelerator grids and out of the thrustor in case 4 represents a maximum possible current or Child's law limit for the given geometry and applied voltages. For an assumed uniform current density across the plasma boundary (which is correct except near the edges) and for an assumed axisymmetric configuration, it can be estimated that, of the 2.58 milliamperes extracted from the plasma (specified condition), roughly 0.9 milliampere is ejected from the thrustor, while the remainder (about 1.7 mA) impinges on the accelerator grid. The calculated current passed by the accelerator system for this case could be approximately 175 milliamperes (35 percent of 500 mA) from a 10-centimeter-diameter thrustor. It has been determined experimentally that 200 milliamperes is about the maximum beam attainable with the given geometry and applied voltages (ref. 3). Attempts to increase the beam current above 200 milliamperes produce greater impingement current with little or no increase in the beam.

The effect of ion current on the potential barrier to backstreaming electrons may be noted by examining cases 3 and 4. In case 3 a minimum potential of -300 volts was observed between the exhaust plasma and the thrustor, providing a barrier to backstreaming electrons. At the higher current level of case 4, however, the ion flow was sufficient to raise the potential level of

this negative potential region appreciably (a slight negative value was measured) thereby approaching a condition in which electron backstreaming could occur. A backstreaming condition exists in the solution of case 2 (i.e., no negative equipotential exists between the thrustor and the exhaust plasma). Experimental data obtained in this region at similar conditions (ref. 17) verifies the onset of electron backstreaming near these conditions.

Effects of net accelerating voltage. - The effect of net accelerating voltage on the location of the ion-chamber-plasma boundary is indicated by a comparison of cases 2 and 3. In both cases, the ion current and the voltage between the plates are the same. As might be expected, higher net accelerating voltages did not affect the upstream plasma boundary, since the total accelerating voltage remained constant. The greater velocities imparted by the higher net accelerating voltage resulted in slightly better focusing of the ion beam. This improved focusing at higher net accelerating voltages is a trend that was noted in reference 3.

Virtual ground. - Although the exhaust-plasma boundary or virtual ground was not located with great accuracy in this study, it is possible to note the general effects of ion-beam current and net-to-total-accelerating voltage ratio on the location of this boundary by a comparison of the solutions for the various cases. Increased ion currents cause this boundary to move closer to the grid system, with the center portion of the boundary disappearing as conditions for electron backstreaming occur. This phenomenon is illustrated by sketch (c).

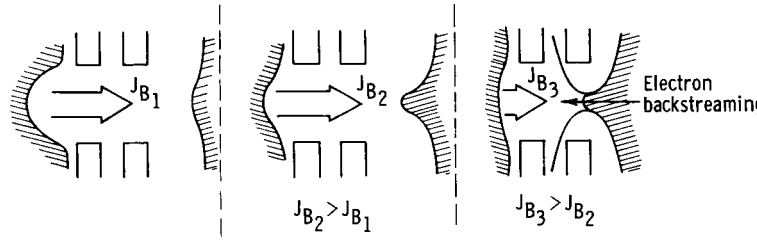

(c)

In the case for which electron backstreaming is predicted, as in case 2, the 0-volt equipotential no longer represents the exhaust-plasma boundary because electron backflow, which is encountered in real thrustors, is not included in this procedure. It might be possible to find this boundary and the electron current extracted from it in order to form a stable boundary by some modification of the technique used for the upstream sheath. The presence of backstreaming, however, is very undesirable for thrustor operation, so the procedure was not considered further.

Charge-exchange ion trajectories. - In three of the four cases considered, the amount of direct ion impingement on the accelerator grid was negligible. It is of interest to determine the trajectories of charge-exchange ions which, in such cases, would be responsible for most of the impingement and resulting erosion of the accelerator grid. Charge-exchange ions are formed in the region of the electrodes when a high-velocity ion exchanges charge with a low-velocity

neutral atom. The resulting low-velocity ion may be accelerated toward and impinge on the accelerator grid. The charge-exchange trajectories were determined by positioning the field-sampling probe (fig. 2) at points in the accelerator system and allowing the probe to move under the influence of the accelerating voltages and the space-charge field (ref. 18). The dashed trajectories in the solutions (figs. 7 to 10) indicate the paths of the charge-exchange ions that impinge on the accelerator. Charge-exchange ions formed upstream of those shown escape from the thrustor, while those formed farther downstream than those shown impinge on the accelerator grid. Those that are formed downstream of the virtual ground, however, would not be expected to impinge but possibly could if any slight accelerating gradient toward the accelerator grid existed within the exhaust plasma.

Of particular interest is the predicted impingement pattern. From figures 7 to 10 it can be seen that a number of the charge-exchange ions strike the sides of the accelerator grid, tending to enlarge the hole. The remainder of the impinging charge-exchange ions are focused toward the center of the downstream face of the accelerator grid. Hence, the expected erosion pattern on a typical accelerator could be as shown in sketch (d). Such erosion patterns have been observed experimentally (ref. 19). Figure 11 is a photograph of the downstream surface of an accelerator grid that was operated for approximately 1300 hours at a total current of 250 milliamperes and a net accelerating potential of 4000 volts. The enlarging of the center holes due to charge-exchange and direct impingement can be noted. The holes were originally all the same size. The pitting between accelerator holes can also be seen.

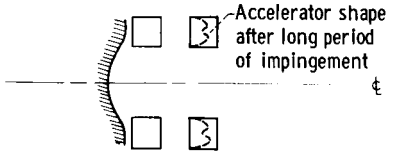

(d)

Accuracy of Solutions

In setting up the original calculation, it was assumed that the optics of one hole in the grids was not influenced significantly by the adjacent holes. It can be seen from the four solutions that there is no interaction in the upstream region. There may be some interaction in the downstream region due to widely diverging trajectories (such as in case 4) that could influence the space-charge distribution. This effect will usually be small, however, because the virtual ground is closer to the accelerator grid than the region in which the majority of the trajectories cross.

While the four cases considered illustrate a number of experimentally observed trends, it is not possible to obtain a detailed quantitative comparison between the analog solutions and experiment without more detailed thrustor diagnostic data than are now available. An alternative method of checking the technique is to use the calculated plasma boundary as a fixed ion emitting surface and calculate the space-charge-limited current flow, potential distribution, and ion trajectories on a digital computer. This was done using the space-charge-flow program reported in reference 14.

The effect of using a two-dimensional model of an axisymmetric hole was studied with the help of a computer program described in reference 20. For

this comparison the space-charge-limited axisymmetric solution was calculated using the two-dimensional plasma boundary as a fixed ion emitter obtained with the analog technique.

Comparison of the digital computer results with those of the analog technique is presented in table II for the four cases. In the first column are listed the specified ion currents used in determining the two-dimensional sheath configuration by the analog technique. Using this sheath as a fixed emitter for the two-dimensional digital computer solution yielded the space-charge-limited currents listed in the second column. These range from 9 to 35 percent below the specified current. In each case, closer agreement could be obtained by shifting the emitter surface downstream by one-half of the mesh spacing between space-charge-simulation pins. The resulting currents are listed in the next column of the table. It therefore appears that the analog technique for locating the sheath is accurate to within one-half of the mesh spacing, which is really the maximum accuracy to be expected.

The difference between space-charge-limited current for the two-dimensional and the axisymmetric cases, using the displaced two-dimensional sheath, is also given in table II. As might be expected, the two-dimensional solution does not produce a good quantitative approximation to the axisymmetric case. Axisymmetric solutions can be obtained with the electrolytic tank by using a tapered tray (ref. 13), but this modification was not within the scope of the present study. It can be concluded from these comparisons that the space-charge-limited current is quite sensitive to the location and form of the emitting plasma boundary.

The ion trajectories and potential distributions obtained by the digital computer for case 1 are presented in figures 12(a) and (b), for the two positions of the emitting surface, and in figure 13 for the axisymmetric case. Comparison of figures 12(a) and (b) shows that the position of the emitter within the one-half mesh spacing had small effect on the ion trajectories. Comparison of figures 12(b) and 13 shows that the axisymmetric case changed the trajectories only slightly but changed the potential distribution considerably. On the grid-hole centerline downstream of the accelerator grid, slightly higher voltages existed (about 20 V) in the digital two-dimensional calculation than in the analog solution. This difference is enough to permit electron back-streaming for the digital solution.

CONCLUDING REMARKS

A general technique has been developed for obtaining the ion optics for the case that the ion source is a thin plasma sheath. The technique was developed using an electrolytic tank analog of the ion accelerating system. No assumption about the location of the sheath is necessary. The parameters that need to be specified are the grid geometry, the applied voltages, the plasma voltages, and the ion current extracted in the vicinity of a single hole in the grids.

Four cases were carried through to completion. These solutions were in qualitative agreement with a number of experimentally observed phenomena and

with solutions obtained from a digital computer program, using the analog-determined plasma boundary as a fixed emitter.

As in the fixed-emitter case, the analog technique developed herein is of value in preliminary evaluation of various grid designs with respect to current capacity, direct ion impingement, and charge-exchange ion impingement for electron-bombardment ion thrustors. More accurate final evaluations would require adapting this technique to digital computers. Once this adaptation is completed, solutions should require much less time than with the present analog technique.

Lewis Research Center,
National Aeronautics and Space Administration,
Cleveland, Ohio, January 26, 1964.

APPENDIX - SYMBOLS

A area, m^2

J current, A

l distance parallel to ion motion, m

N total number of stream tubes

V potential, V

ϵ_o permittivity of free space, $8.85 \times 10^{-12} \frac{C^2}{N\text{-}m^2}$

ρ space charge density, C^2/m^3

Subscripts:

B beam

i number of a specific trajectory stream tube

REFERENCES

1. Kaufman, H. R.; and Reader, P. D.: Experimental Performance of Ion Rockets Employing Electron-Bombardment Ion Sources. Prog. in Astronautics and Rocketry, Vol. 5, Academic Press, Inc., 1961, pp. 3-20.

2. Kaufman, Harold R.: An Ion Rocket With an Electron-Bombardment Ion Source. NASA TN D-585, 1961.

3. Kerslake, William R.: Accelerator Grid Tests on an Electron-Bombardment Ion Rocket. NASA TN D-1168, 1962.

4. Kerslake, William R.; and Pawlik, Eugene V.: Additional Studies of Screen and Accelerator Grids for Electron-Bombardment Ion Thrustors. NASA TN D-1411, 1963.

5. Mickelson, William R.: Theoretical Performance of Electrostatic Thrustors With Analytic Space-Charge Flows. NASA TR R-174, 1963.

6. Staggs, John F.: An Electrolytic-Tank Analog for Two-Dimensional Analysis of Electrostatic-Thrustor Optics. NASA TN D-2803, 1965.

7. Stuhlinger, E.: Possibilities of Electrical Space Ship Propulsion. Proc. Int. Astronautical Cong., Innsbruck, 1954, pp. 100-119.

8. Stuhlinger, E.: Electrical Propulsion Systems for Space Ships with Nuclear Power Sources, pts. I-III. J. Astronautics, vol. 2, no. 4, 1955, pp. 149-152; vol. 3, no. 1, 1956, pp. 11-14; vol. 3, no. 2, 1956, pp. 33-36.

9. Eckhardt, W. O.; et al.: Research on Ion Beam Formation from Plasma Sources. Paper No. 64-8, AIAA, 1964.

10. Kaufman, Harold R.: The Neutralization of Ion Rocket Beams. NASA TN D-1055, 1961.

11. Domitz, Stanley: Experimental Evaluation of a Direct-Current Low-Pressure Plasma Source. NASA TN D-1659, 1963.

12. Hollway, D. L.: The Determination of Electron Trajectories in the Presence of Space Charge. Australian J. of Phys., vol. 8, no. 1, Mar. 1955, pp. 74-89.

13. Van Duzer, T.; and Brewer, G. R.: Space-Charge Simulation in and Electrolytic Tank. J. Appl. Phys., vol. 30, no. 3, Mar. 1959, pp. 291-301.

14. Hamza, Vladimir; and Richley, Edward A.: Numerical Solution of Two-Dimensional Poisson Equation: Theory and Application to Electrostatic-Ion-Engine Analysis. NASA TN D-1323, 1962.

15. Reader, Paul D.: Investigation of a 10-Centimeter-Diameter Electron-Bombardment Ion Rocket. NASA TN D-1163, 1962.

16. Kerslake, William R.: Charge-Exchange Effects on the Accelerator Impingement of an Electron-Bombardment Ion Rocket. NASA TN D-1657, 1963.

17. Nakanishi, Shigeo; Pawlik, Eugene V; and Baur, Charles W.: Experimental Evaluation of Steady-State Control Properties of an Electron-Bombardment Ion Thrustor. NASA TN D-2171, 1964.

18. Brewer, G.: On the Nature of Leakage Currents in Cesium Contact Ion Engines. Research Rept. No. 281, Hughes Res. Labs., Aug. 1963.

19. Reid, G. C.; Barcatta, F. A.; Sohl, G.; and Speiser, R. C.: Ion Rocket System Research and Development. EOS Rept. No. 4920-Q-2, Electro-Optical Systems, Inc., Sept. 20, 1964.

20. Hamza, Vladimir (With appendix C by Carl D. Bogart): Numerical Solution of Axially Symmetric Poisson Equation: Theory and Application to Ion-Thrustor Analysis. NASA TN D-1711, 1963.

TABLE I. - SPECIFIED ELECTRICAL PARAMETERS

Case	Screen voltage, V	Accel-erator voltage, V	Ion current per hole, mA	Total beam current, mA	Solution given in figure -
1	2500	-833	0.258	50	7
2	2500	-833	.600	128	8
3	1666	-1666	.600	128	9
4	1666	-1666	2.580	500	10

TABLE II. - COMPARISON OF ANALOG AND DIGITAL COMPUTER RESULTS

Case	Specified ion current per hole, mA	Digital computer values for space-charge-limited current per hole, mA			Percent variation between -		
		A; Plasma boundary as deter-mined by analog	B; Plasma boundary moved down-stream one-half mesh spacing	C; Axisymmetric geometry; plasma boundary down-stream one-half mesh spacing	Specified value and computer result A	Specified value and computer result B	Computer results B and C
1	0.258	0.196	0.262	0.223	-24.0	1.5	-14.9
2	.600	.458	.575	.378	-23.7	-4.2	-34.2
3	.600	.392	.552	.371	-34.7	-8.0	-32.8
4	2.58	2.35	2.61	2.83	-8.9	1.5	8.4

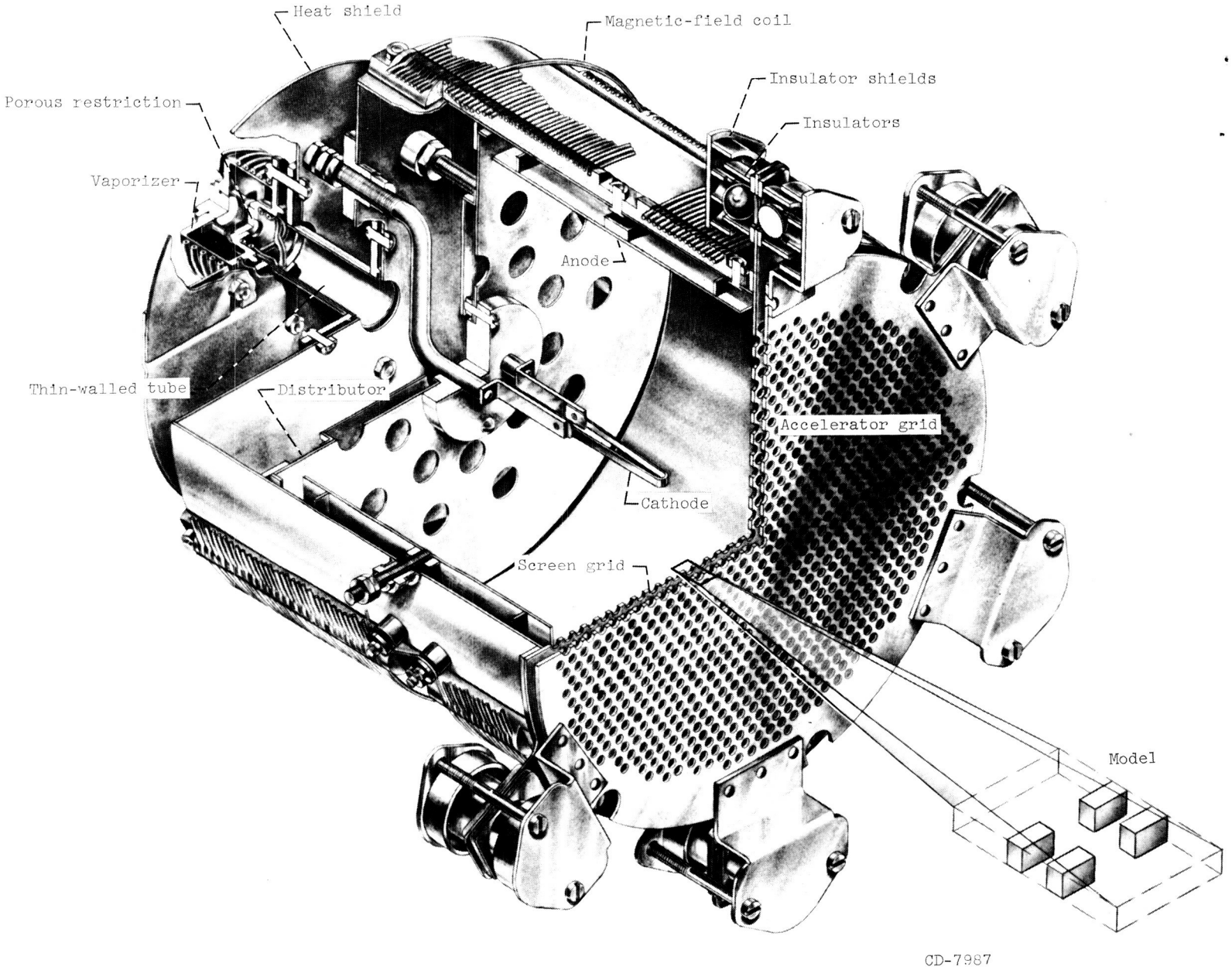

Figure 1. - Cutaway view of 20-centimeter-diameter electron-bombardment ion thrustor.

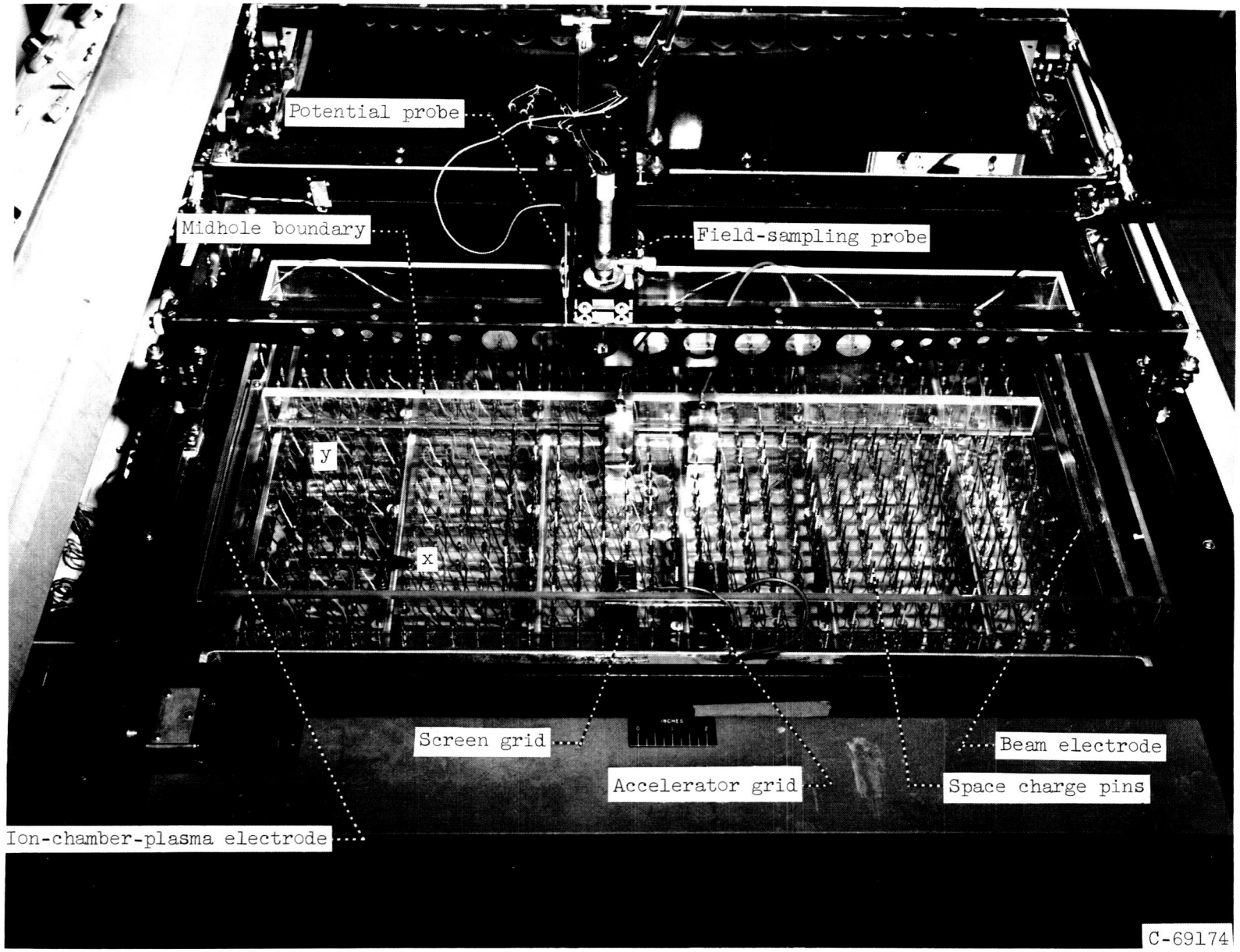

Figure 2. - Model accelerator system and boundary strips installed in the electrolytic tank.

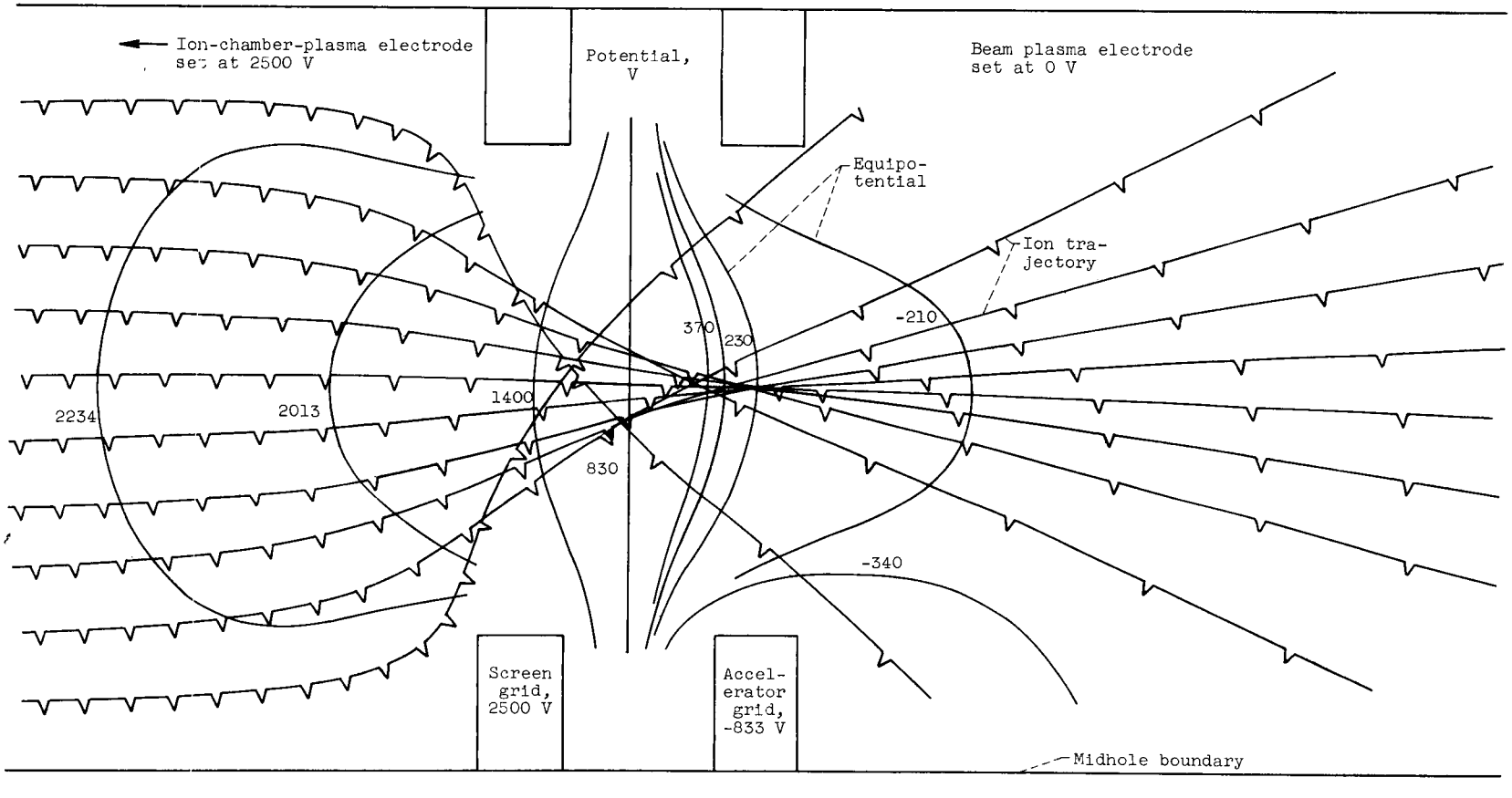

Figure 3. - Laplace solution for case 1.

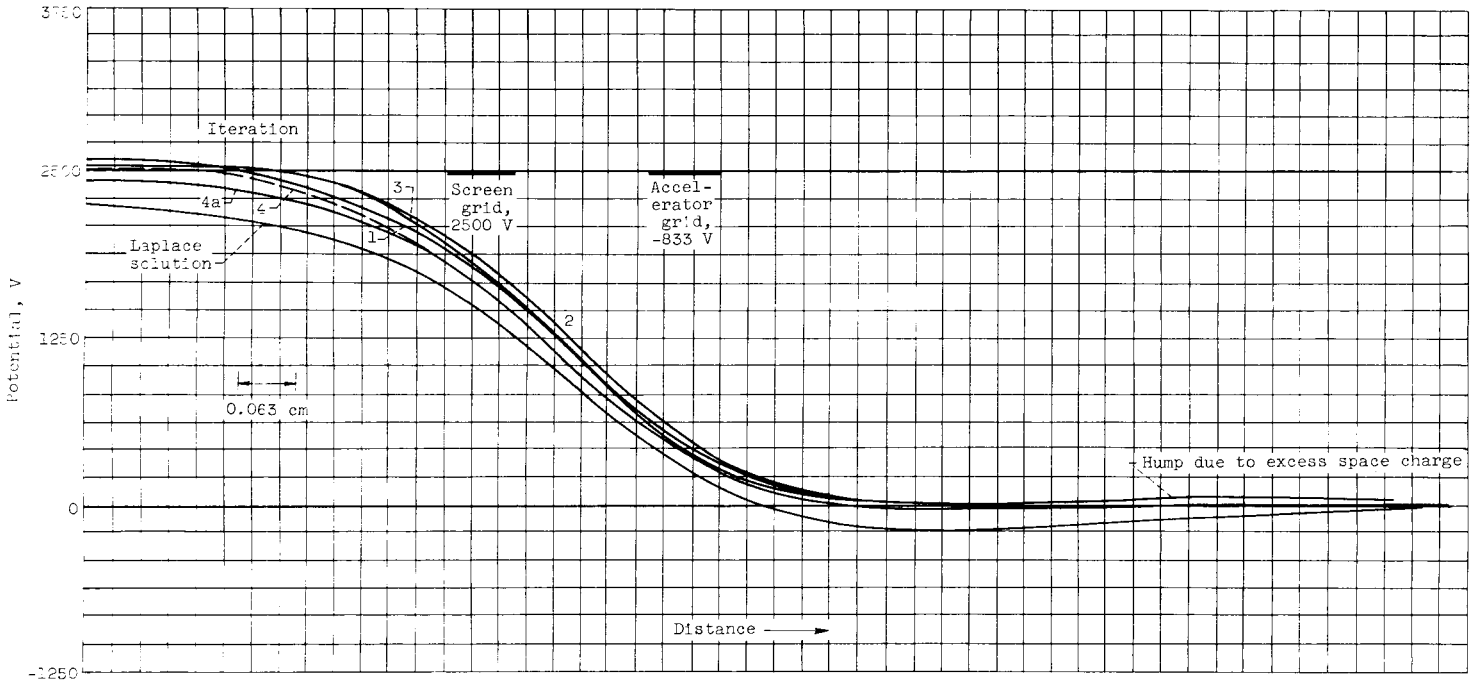

Figure 4. - Centerline potential distribution for first four iterations of case 1.

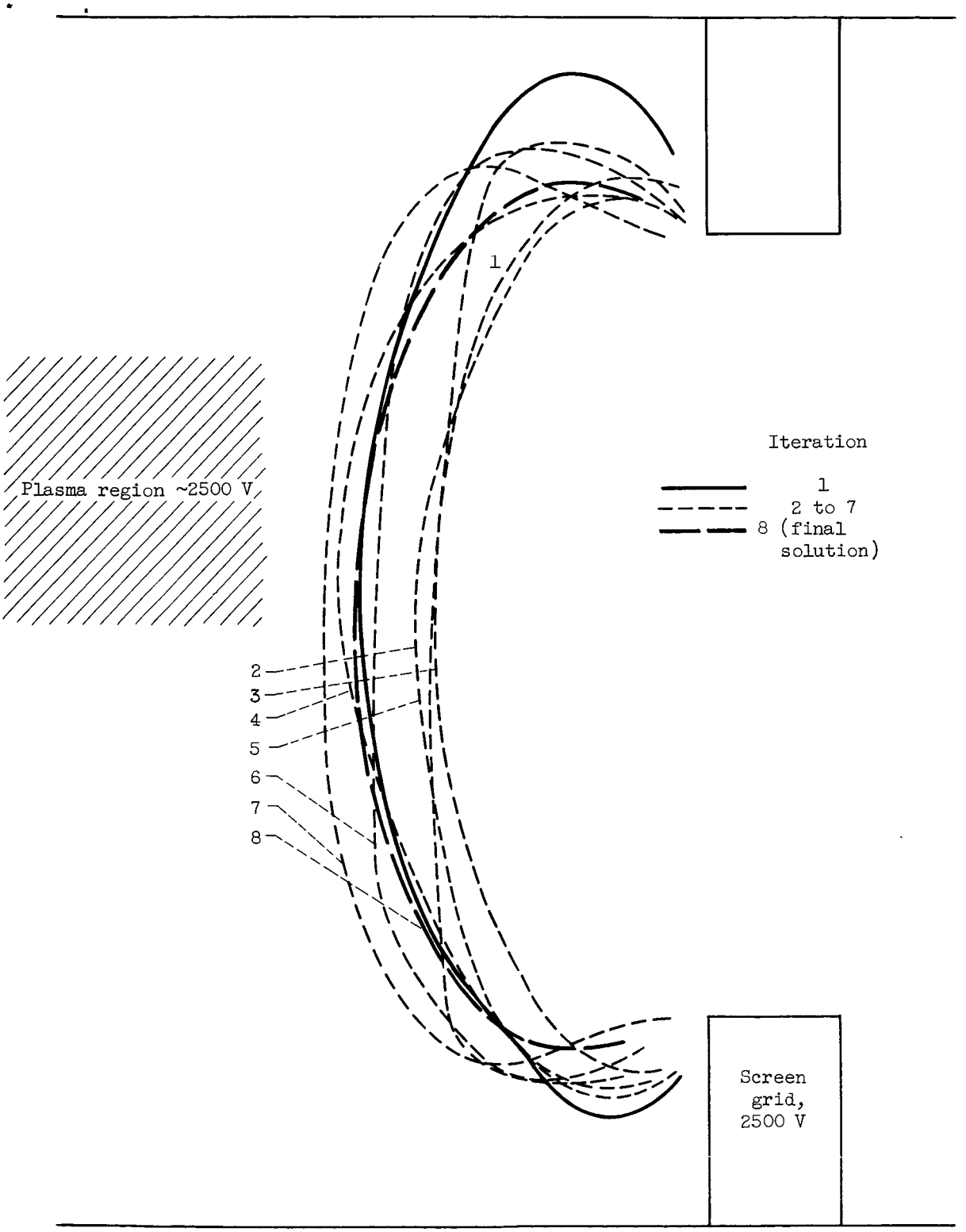

Figure 5. - Equipotential lines representing successive approximations to plasma boundary for case 1.

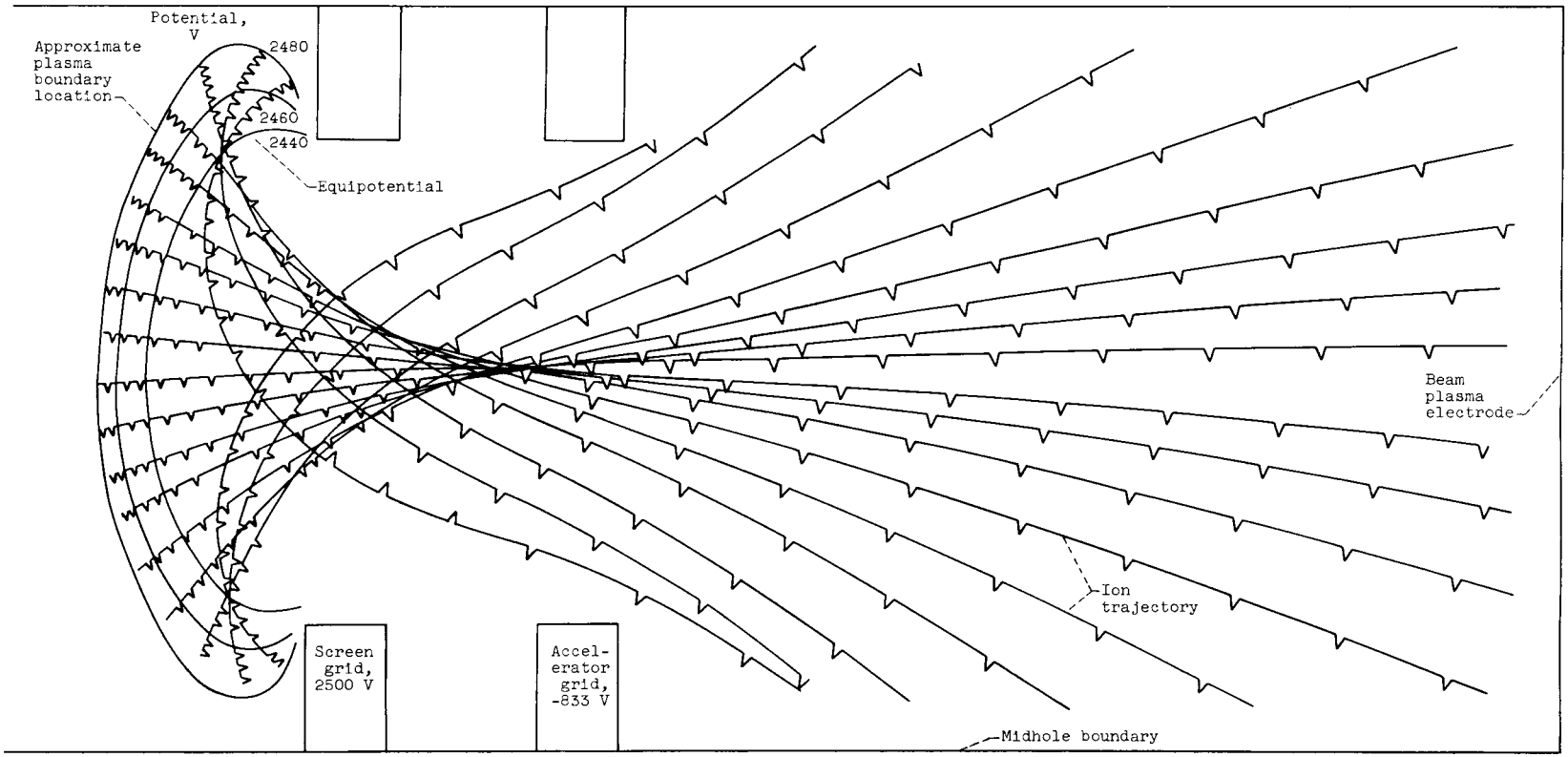

Figure 6. - First iteration for case 1.

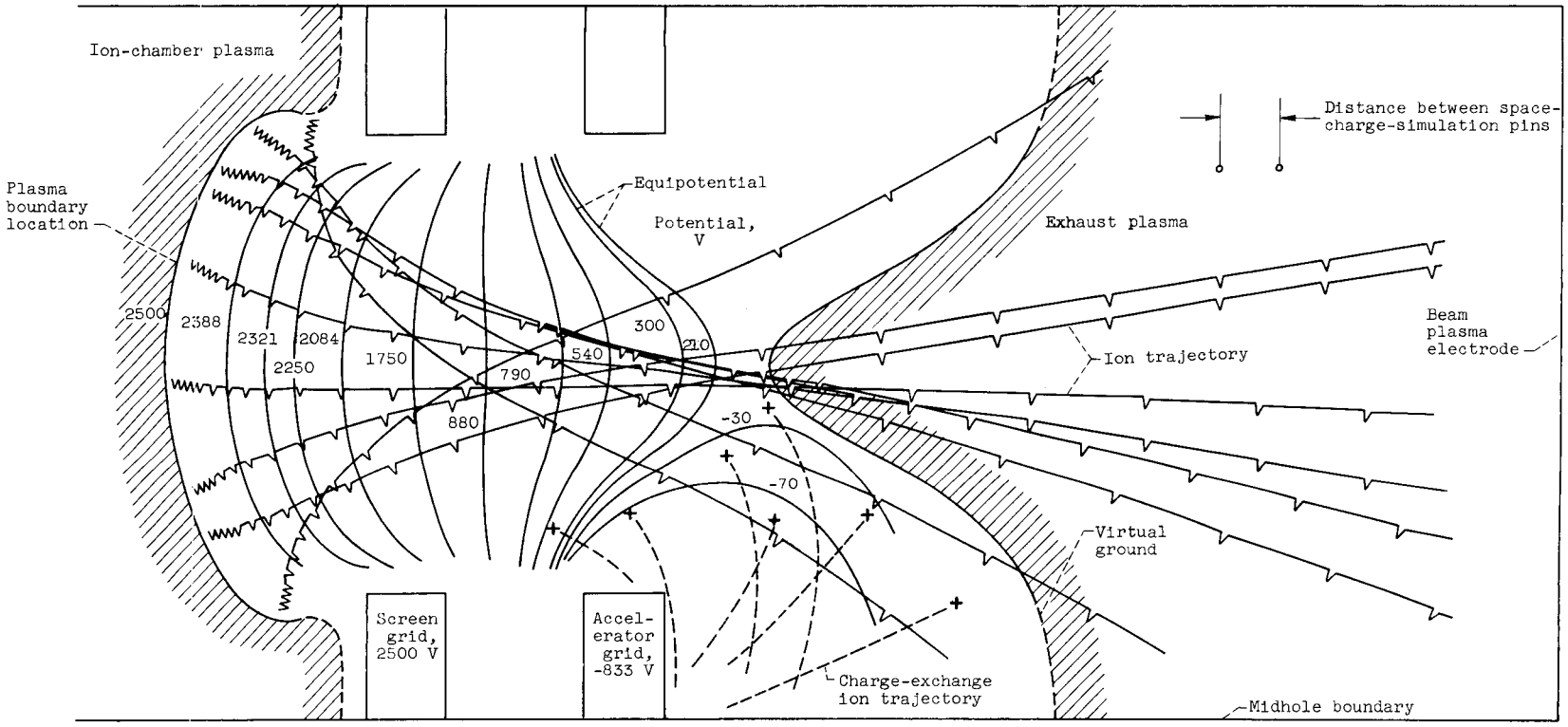

Figure 7. - Solution for case 1. Current, 0.258 milliampere; potentials as indicated.

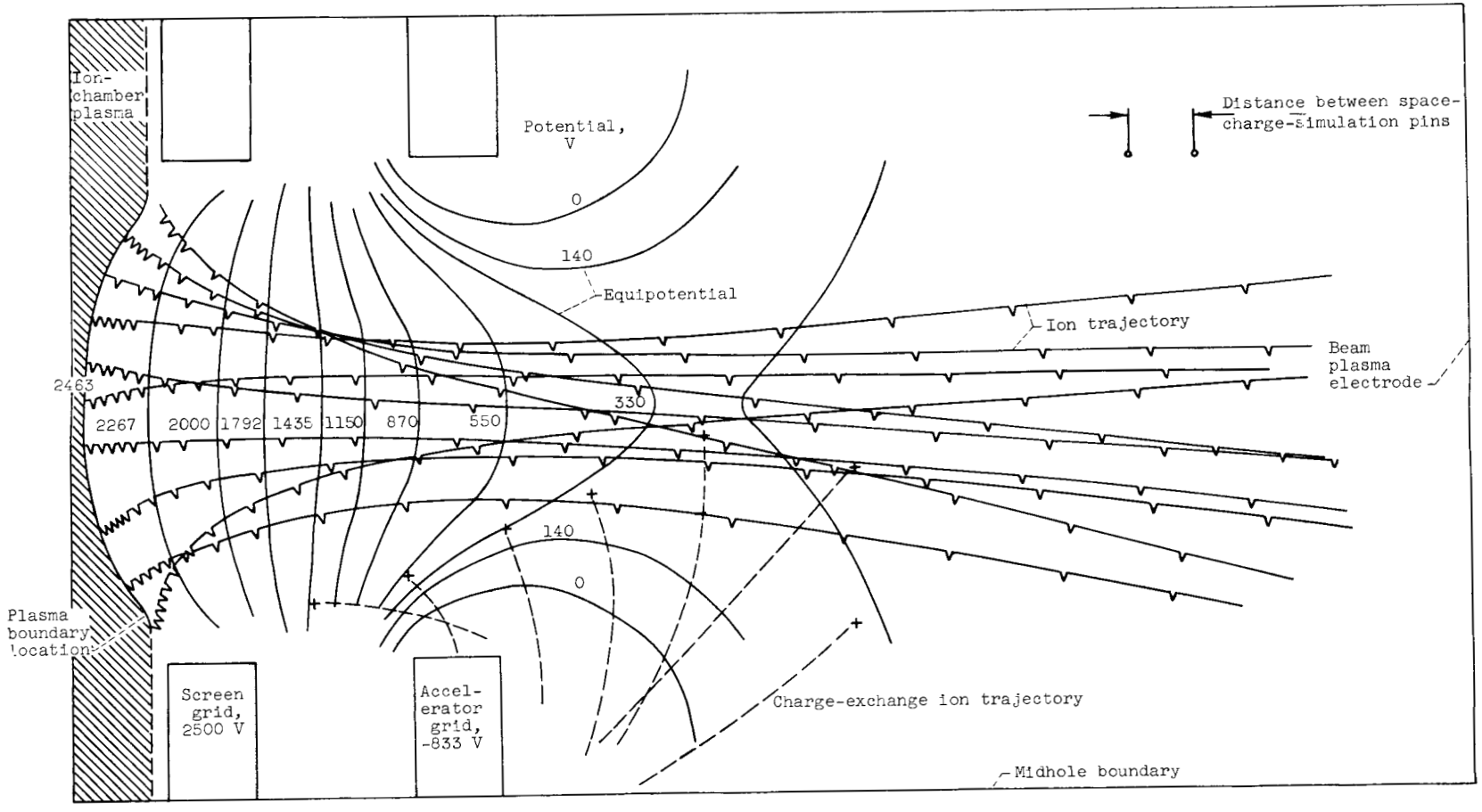

Figure 8. - Solution for case 2. Current, 0.600 milliampere; potentials as indicated.

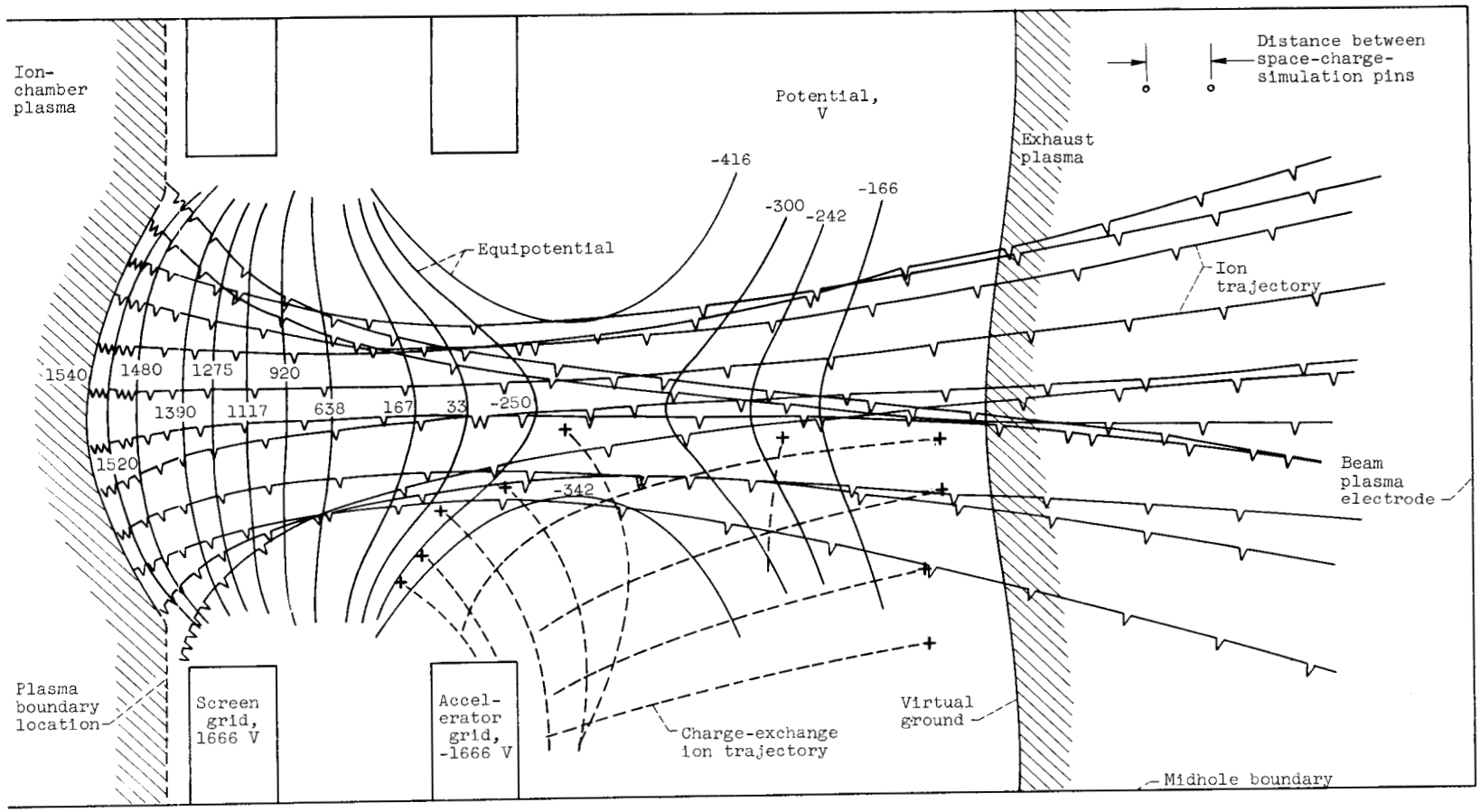

Figure 9. - Solution for case 3. Current, 0.600 milliampere; potentials as indicated.

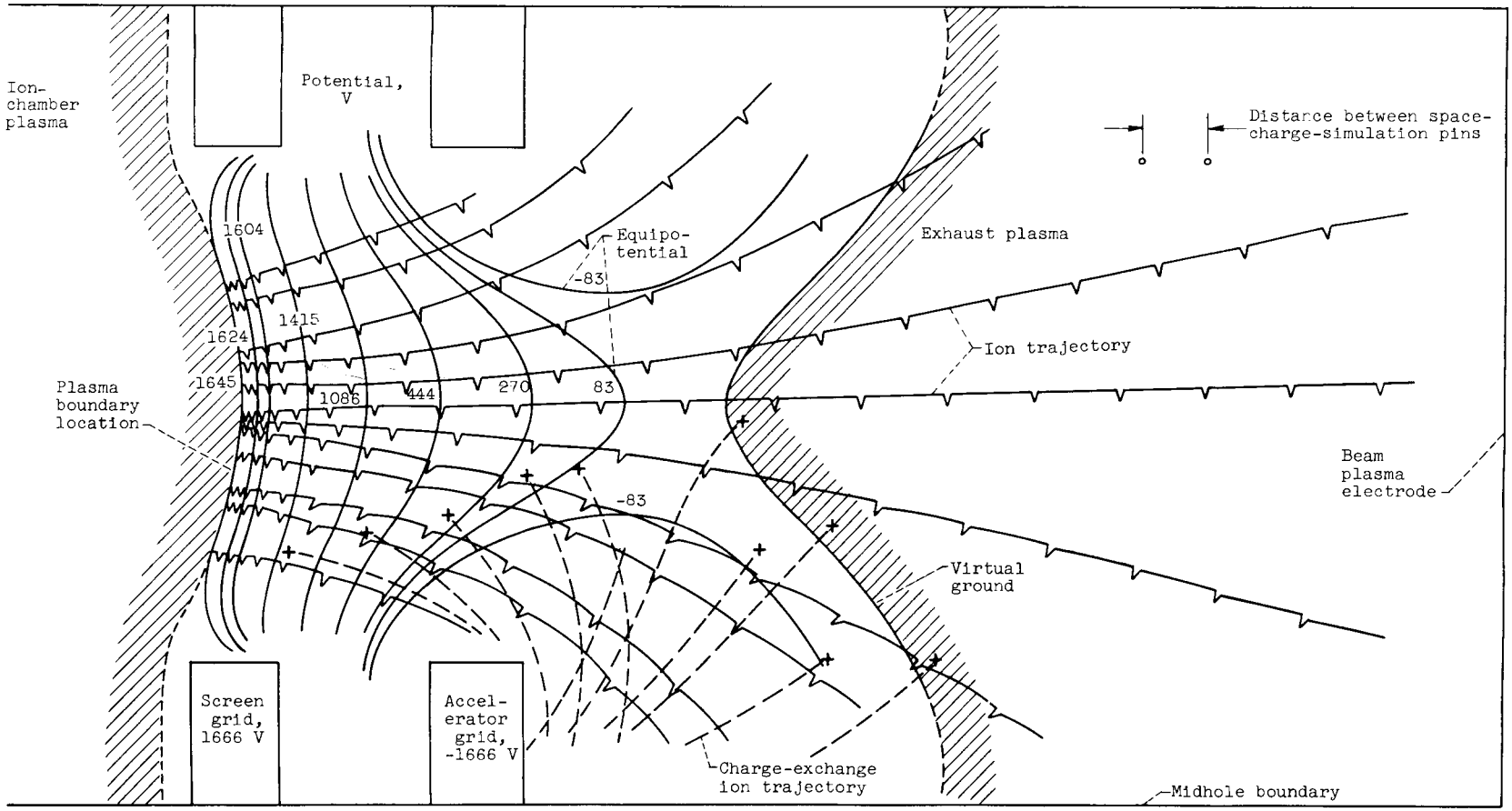

Figure 10. - Solution for case 4. Current, 2.58 milliampere; potentials as indicated.

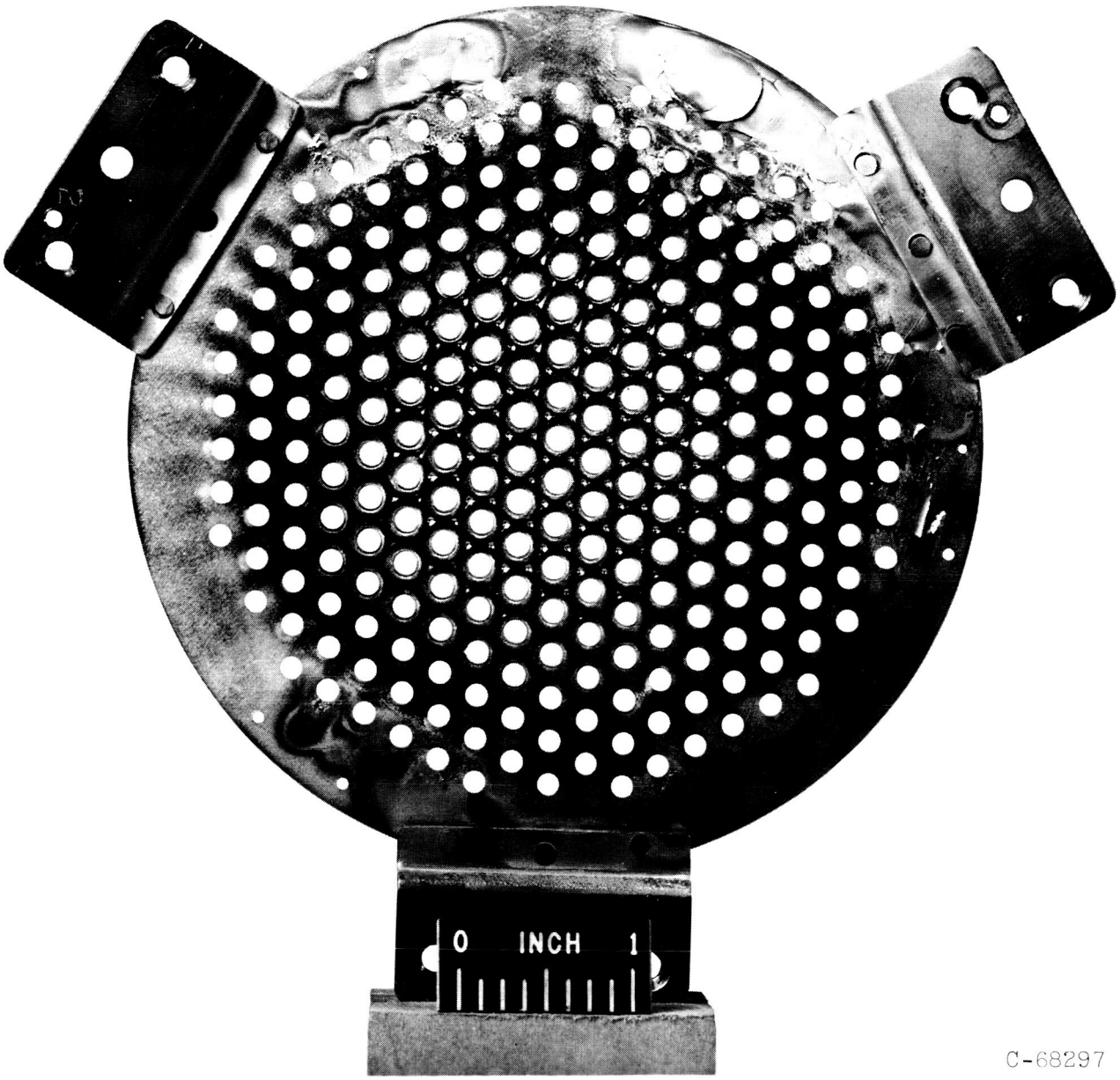

C-68297

Figure 11. - Downstream face of accelerator grid from electron-bombardment ion thrustor after 1300 hours of operation. Screen potential, 4000 volts; accelerator potential 1000 volts; beam current, 0.250 ampere; average current per hole, 1.0 milliampere.

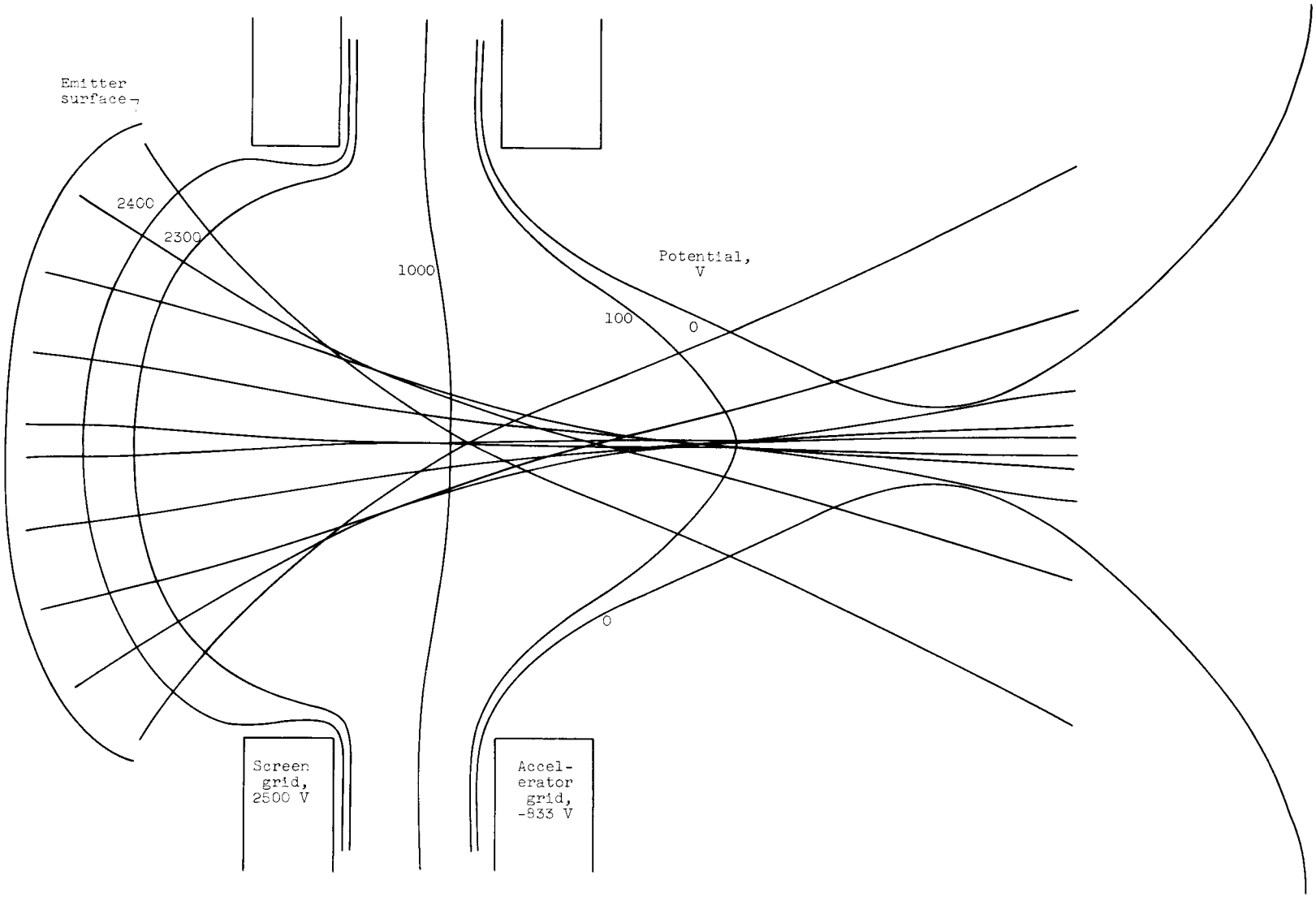

(a) Sheath at same position as for analog solution.

Figure 12. - Digital computer solution for case 1.

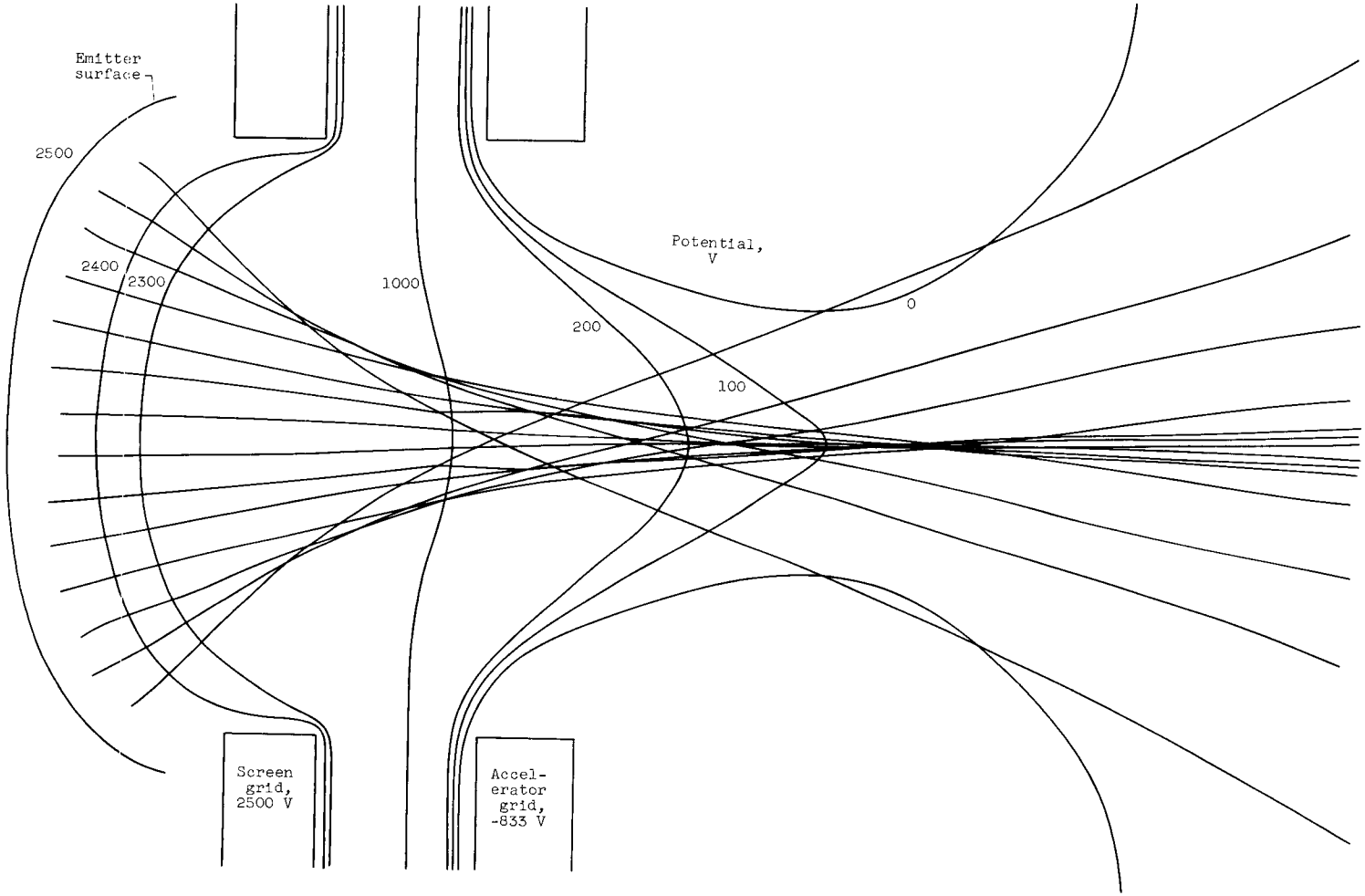

(b) Sheath moved forward one-half mesh spacing.

Figure 12. - Concluded. Digital computer solution for case 1.

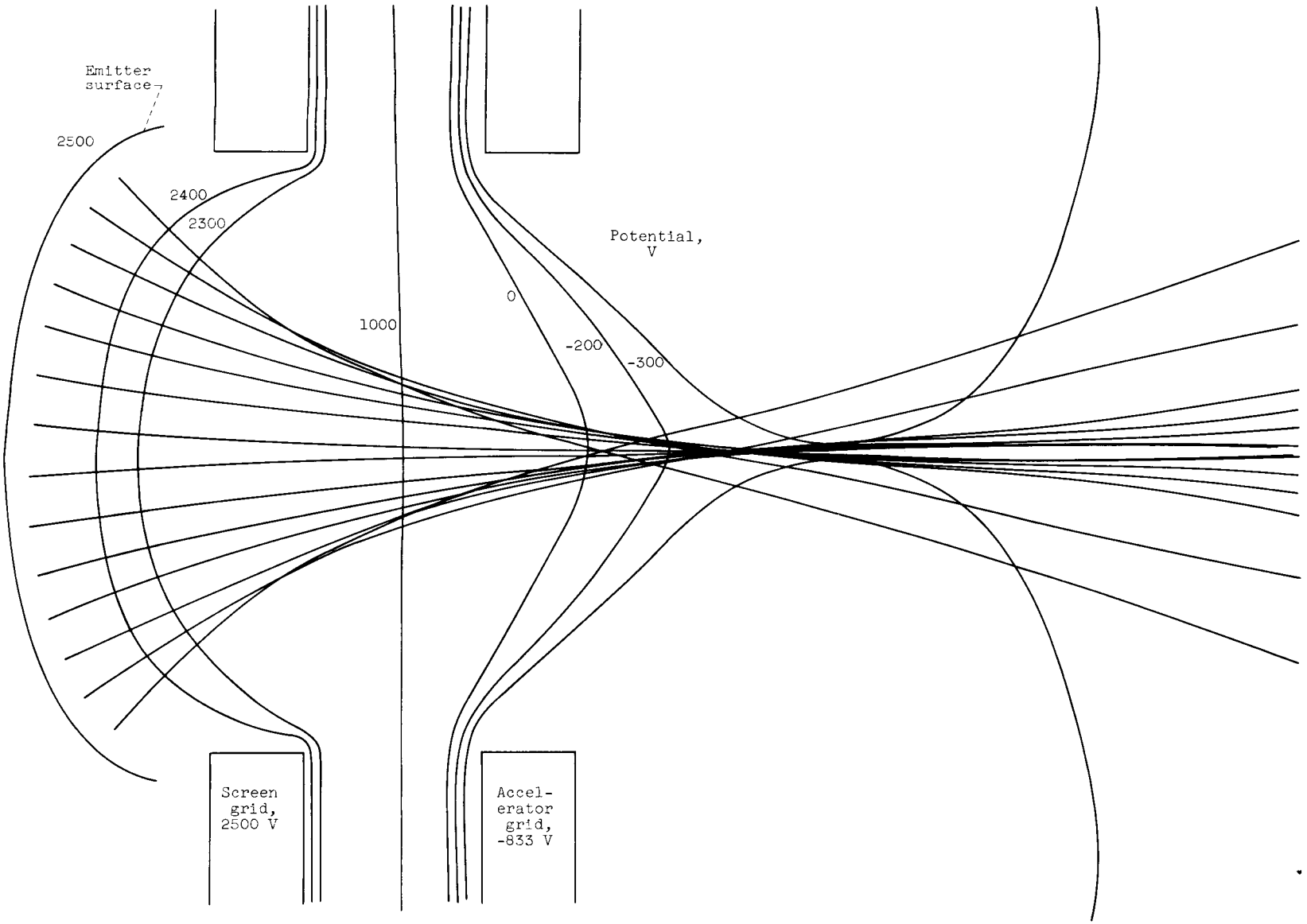

Figure 13. - Digital computer solution for axisymmetric geometry, otherwise similar to case 1. Sheath moved forward one-half mesh spacing.